Anal Bioanal Chem (2014) 406:3887–3894
DOI 10.1007/s00216-013-7510-0

RESEARCH PAPER

Detection of silver nanoparticles in parsley by solid sampling high-resolution–continuum source atomic absorption spectrometry

Nadine S. Feichtmeier · Kerstin Leopold

Received: 13 October 2013 / Revised: 6 November 2013 / Accepted: 11 November 2013 / Published online: 1 December 2013

Abstract In this work, we present a fast and simple approach for detection of silver nanoparticles (AgNPs) in biological material (parsley) by solid sampling high-resolution–continuum source atomic absorption spectrometry (HR-CS AAS). A novel evaluation strategy was developed in order to distinguish AgNPs from ionic silver and for sizing of AgNPs. For this purpose, atomisation delay was introduced as significant indication of AgNPs, whereas atomisation rates allow distinction of 20-, 60-, and 80-nm AgNPs. Atomisation delays were found to be higher for samples containing silver ions than for samples containing silver nanoparticles. A maximum difference in atomisation delay normalised by the sample weight of 6.27±0.96 s mg^{-1} was obtained after optimisation of the furnace program of the AAS. For this purpose, a multivariate experimental design was used varying atomisation temperature, atomisation heating rate and pyrolysis temperature. Atomisation rates were calculated as the slope of the first inflection point of the absorbance signals and correlated with the size of the AgNPs in the biological sample. Hence, solid sampling HR-CS AAS was proved to be a promising tool for identifying and distinguishing silver nanoparticles from ionic silver directly in solid biological samples.

Keywords Silver nanoparticle detection · High-resolution–continuum source atomic absorption spectrometry · Solid sampling · Food analysis

Published in the topical collection *Characterisation of Nanomaterials in Biological Samples* with guest editors Heidi Goenaga-Infante and Erik H. Larsen.

Electronic supplementary material The online version of this article (doi:10.1007/s00216-013-7510-0) contains supplementary material, which is available to authorized users.

N. S. Feichtmeier · K. Leopold (✉)
Institute of Analytical and Bioanalytical Chemistry, University of Ulm, Albert-Einstein-Str. 11, 89081 Ulm, Germany
e-mail: kerstin.leopold@uni-ulm.de

Introduction

Nanomaterials have received a lot of attention in industry and technology due to their unique physicochemical properties. Metal nanoparticles are particularly useful as catalysts, optical sensors, in textile engineering, electronics, optics, biosensing and in medical applications [1]. Due to these broad fields of application, the Nanotechnology Working Group estimated that the worldwide market for nanotechnology products will reach $1 trillion by 2015 [2]. Especially silver nanoparticles (AgNPs) found massive applications as bactericidal or therapeutic agent in consumer products, such as personal care products, clothing, cosmetics, dressings, etc. [3–5]. Accordingly, AgNP-containing consumer products represent about 30 % of all products registered in nanoproduct databases [6]. In recent years, AgNPs were increasingly applied in food industry and research, e.g. for impregnation of fridges, food boxes and cutting boards in order to inhibit the development of biofilm due to their antimicrobial properties [7–9]. Besides the positive effect of preventing bacterial growth, the risk of AgNPs entering human food and their distribution via the water cycle occurs. In this context, Huang et al. [10] could demonstrate the migration of AgNPs from commercially available fresh food containers into a simulated food-solution. This observation is alarming regarding the well-documented toxic effects of AgNPs for several organisms in recent years [11–13]. AgNPs are not only toxic for aquatic organisms, like, e.g. zebrafish [14], but also for macrophages, human T cells and rat liver cells [15–17]. Medina et al. [18] could show that AgNPs can pass through the epithelia of the respiratory tract and enter directly the blood stream and can even be taken up by nerve endings and cross the central nervous system [19]. Toxicity and sites of action differ when comparing ionic silver species with AgNPs. Ionic silver crosses biological barriers and reaches almost every organ and/or cell, while nanoparticulate silver is taken up

specifically in cellular and sub-cellular locations. Here, the potential dissolution of AgNPs would release high local ionic concentrations with unforeseen consequences [6]. Hence, distinction between ionic silver and AgNPs is a crucial issue when assessing the potential risks arising from AgNPs-containing products that come into contact with food.

There is a broad variety of analytical techniques for detection of silver in food samples, like conventional or single particle inductively coupled plasma mass spectrometry (ICP-MS), inductively coupled plasma optical emission spectrometry, surface plasmon resonance-based sensor or graphite furnace atomic absorption spectrometry [20–24]. Most techniques require the transformation of food samples into a liquid sample, e.g. by enzymatic digestion, acidic extraction, extraction with HEPES or cloud point extraction with subsequent microwave digestion [20, 23–25]. However, in order to distinguish between particulate and soluble forms of silver, suitable sample pretreatment, separation methods and/or data evaluation must be developed. Often species-specific extraction methods are applied, for instance, acidic extraction for the analysis of silver nanoparticles in pears [22] or the applied measurement technique allows distinction of NPs from ionic species, e.g. by application of single particle ICP-MS [21]. For detection of AgNPs in acidified homogenates from liver of rainbow trout, graphite furnace atomic absorption spectrometry was applied providing distinction of AgNPs from silver ions by interpretation of the data at different atomisation temperatures [24]. As a drawback, all these methods are elaborative and time-consuming and are therefore not useful for screening of large sample series, which is required in food and environmental analysis. Hence, the development of approaches for direct investigation of solid samples omitting any sample pretreatment is meaningful.

Therefore, the objective of this study was to develop a method for direct detection of AgNPs in a solid biological sample by application of solid sampling high-resolution–continuum source atomic absorption spectrometry. A new strategy in evaluating the obtained absorbance signals was developed implementing atomisation delay and atomisation rate as new tools for distinguishing AgNPs from ionic silver and sizing AgNPs, respectively. For this purpose, three furnace program parameters, atomisation temperature, heating rate and pyrolysis temperature, were optimized in a 3^3 factorial experimental design. For proof of principle, AgNP-spiked parsley was used as simulated food/biological sample.

Materials and methods

Chemicals

All solutions were prepared using high-purity Milli-Q water (Millipore, Billerica, USA) and 65 % nitric acid (p.a., Merck, Darmstadt, Germany) for acidification. Silver standard solution ($AgNO_3$ in 2 % *w/w* HNO_3, c(Ag)=1,000 mg L^{-1}, Sigma Aldrich, St. Louis, USA) was used for the preparation of simulated sample of plant tissue containing Ag^+ ions. Hydrosols of citrate-stabilised silver nanoparticles (AgNPs) of different sizes (20, 40, 60, 80 nm) were purchased from BBI Solutions (Cardiff, UK) and used without any further treatment for preparation of AgNP-containing plant tissue.

Preparation of simulated samples

Simulated samples were prepared by spiking commercially available dried parsley with defined volumes of Ag^+ standard solutions and/or AgNPs hydrosol. First, plant tissue was homogenised by manually milling the parsley with an agate pestle. Then, 1 mL of 100 μg L^{-1} AgNPs (size, 20, 40, 60 or 80 nm, respectively) and 1 mL of 100 μg L^{-1} Ag^+ standard solution (1,000 mg L^{-1}) were added to 0.3 g of fine-grained homogenised parsley, resulting in a final concentration of 0.7 μg g^{-1} in all plant samples. The obtained slurry was mixed, and the samples were then placed in a drying oven at 80 °C for about 24 h until complete dehydration. After that, the dried tissues were again homogenised by milling. In order to evaluate the homogeneity of the prepared samples ten aliquots of each sample were investigated by solid sampling atomic absorption spectrometry measurements for silver detection.

Silver detection by solid sampling high-resolution–continuum source atomic absorption spectrometry

The detection of silver was performed by high-resolution–continuum source atomic absorption spectrometry (HR-CS AAS) using a *ContrAA 600* (Analytik Jena AG, Jena, Germany), equipped with a graphite furnace atomisation unit and an auto sampler SSA 600 for solid sampling with integrated microbalance or alternatively, with auto sampler AS52s for liquid sampling. The AAS was operated with 99.999 % Argon (MTI, Neu-Ulm, Germany). Data evaluation was achieved with the software ASPECT CS 1.5.6.0 (Analytik Jena AG). Atomic absorption of silver was detected at 328.07 nm, which is the most sensitive atomic line for silver. The temperature program for the graphite furnace proposed by the instrument's supplier for liquid sampling is given in Table 1; for the detection of Ag in the solid samples, optimisation of pyrolysis and atomisation temperature as well as of atomisation heating rate was performed.

Concentration of commercially available AgNPs hydrosols was determined by liquid sampling HR-CS AAS after calibration in a range from 15 to 150 μg L^{-1}. The concentrations found were 7.37 mg L^{-1} for 20-nm AgNPs hydrosol, 7.18 mg L^{-1} for 40-nm AgNPs hydrosol, 7.04 mg L^{-1} for

Table 1 Graphite furnace program for the detection of silver by HR-CS AAS as recommended by the instrument's supplier

Step	Temperature [°C]	Heating rate [°C s^{-1}]	Hold time [s]
Drying I	80	5	20
Drying II	130	10	20
Pyrolysis	300	300	20
Auto-zero	300	0	5
Atomisation	1,600	1,500	7
Cleaning	2,450	500	4

60-nm AgNPs hydrosol and 4.50 mg L^{-1} for 80-nm AgNPs hydrosol.

Results and discussion

Representation of test material

Development of the proposed method was performed applying silver-spiked parsley samples as a test material. Silver ions and/or silver nanoparticles of a defined particle size were added as a solution or hydrosol to the biological material. This strategy provides well-defined biological samples and gives therefore reproducible results that are required in order to develop and optimise the analysis method. However, it can be expected that, in real samples, e.g. food, which comes into contact with silver due to its preservation in silver nanoparticle-containing packages, AgNPs and/or Ag^+ ions are adsorbed on the sample surface just like in the simulated samples that were prepared and studied in this work. Moreover, application of the proposed analytical method to barley samples that were obtained after exposure and uptake of gold nanoparticle by the living organism revealed no significant differences in absorption signals and atomisation delays in comparison to samples that were simulated, i.e. where the barley plant material was spiked with gold nanoparticles after harvesting. Hence, we think that the prepared parsley samples are suitable test material for proof of concept of the proposed analytical method.

Investigation of homogeneity of prepared solid samples

The homogeneity of the prepared parsley samples containing either ionic silver (Ag^+) or a mixture of AgNPs/Ag^+ is essential in order to receive meaningful data for interpretation. Hence, homogeneity of all samples has been thoroughly checked by performing replicated solid sampling HR-CS-AAS measurements. For this purpose, at least ten aliquots of approximately 50 to 250 μg of each sample were investigated. Initial experiments were conducted applying the furnace program recommended by the instrument's supplier (see Table 1; results are presented in Electronic supplementary material Fig. S1) and were repeated after final optimisation of the furnace parameters as described below (see Fig. 1). The results prove a fairly good homogeneity of the prepared samples, i.e. linear correlation between absorbance and sample weights, as according to the law of Lambert-Beer. Furthermore, the

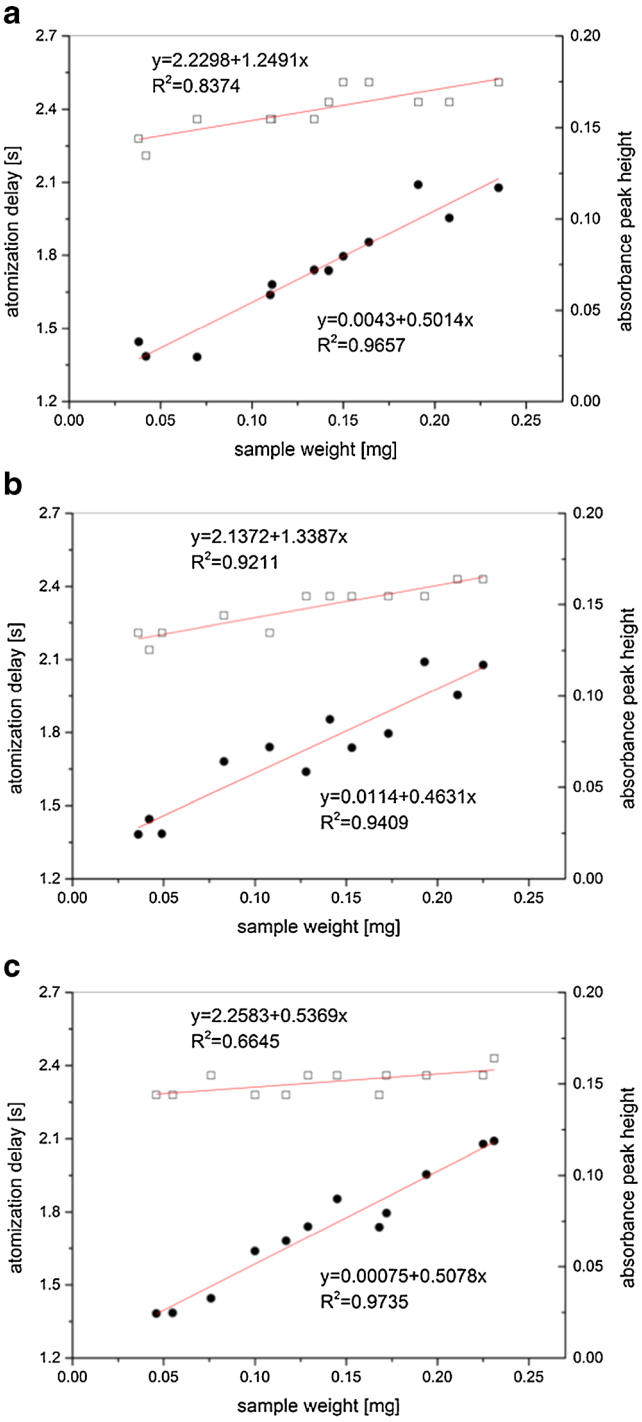

Fig. 1 Absorbance (*black circle*) and atomization delay (*white square*) for parsley samples spiked with **a** ionic silver, **b** a mixture of ionic silver and 20-nm AgNPs and **c** a mixture of ionic silver and 80-nm AgNPs as a function of sample weight obtained by application of furnace program #5

optimal sample weight range was found to be between 100 and 200 μg in regard to reproducibility of the absorbance value.

Strategy development for interpretation of measurement data

In atomic absorption spectrometry, the absorbance signal is detected over a given time interval, typically a few seconds, in which complete atomisation of the studied element occurs. Optimum atomisation temperature is of course element-specific, and atomisation rate depends on the composition of the sample matrix. However, standard interpretation of signals obtained by AAS comprises quantitative evaluation of the absorbance peak by measuring its height or area. In this work, it will be shown that further interpretation of the signal allows indication of silver species, i.e. nanoparticles or ionic silver, directly in the solid sample. For this purpose, two different evaluation strategies were developed:

(A) Determination of the atomisation delay (t_{ad}), i.e. the time period from starting the atomisation step until the peak maximum is found;
(B) Determination of the atomisation rate (k_{at}), calculated as the slope of the polynomial fitted curve at the first inflection point.

Figure 2 presents an exemplary absorbance signal obtained for Ag^+-containing parsley and illustrates these strategies.

The obtained data for absorbance and atomisation delay, as presented in Fig. 1, show linear correlation with sample weight, i.e. both parameters increase with rising masses. This effect is to be expected due to the fact that a higher amount of sample causes (a) a larger number of absorbing silver atoms in the atomisation unit and (b) a slower heat transfer. Hence, in order to evaluate whether t_{ad} can be used to distinguish silver nanoparticles from ionic silver species, all values were normalised by means of division by sample weight (m_s). The evaluation of normalised atomisation delay ($t_{nad}=t_{ad}/m_s$) has been used as crucial parameter to optimise the furnace program for best distinction between AgNPs and ionic silver species. For this purpose, the differences in t_{nad} of ionic silver and nanoparticulate silver, signified as "Δt" (with $\Delta t = t_{nad}(Ag^+) - t_{nad}(AgNPs/Ag^+)$) were calculated for all experiments, whereas evaluation of the atomisation rate was applied in order to assess whether conclusions on different nanoparticle sizes are possible.

Optimisation of furnace program with multivariate approach

Three variables were expected to be most important in order to optimise the graphite furnace program for distinguishing AgNPs from ionic silver in parsley: (1) atomisation temperature; (2) atomisation heating rate and (3) pyrolysis temperature. Therefore, a multivariate approach was used applying the 3^3 factorial design, as given in Table 2. The selected temperature ranges for multivariate experiments derive from the following considerations: For solid sampling, generally higher atomisation temperatures and heating rates are preferable than for liquid samples, since the analyte interacts stronger with the sample matrix [26]. At the same time, higher pyrolysis temperatures are needed in order to minimise matrix effects. Hence, lowest tested values are based on the recommendations given by the instrument's supplier for liquid samples (cf. Table 1).

Application of 700 °C for pyrolysis showed very small atomisation delays and/or very broad peaks and did not allow expedient evaluation of atomisation delay or rate. Accordingly, meaningful results were obtained for 18 variations of furnace programs applied to five differently spiked parsley samples (Ag^+; 20-nm AgNPs/Ag^+, 40-nm AgNPs/Ag^+, 60-nm AgNPs/Ag^+, 80-nm AgNPs/Ag^+, respectively; see Electronic supplementary material Table S1). For parsley samples spiked with Ag^+, the values for the normalised atomisation delay (t_{nad}) ranged from 13.02 to 28.89 s mg^{-1} depending on

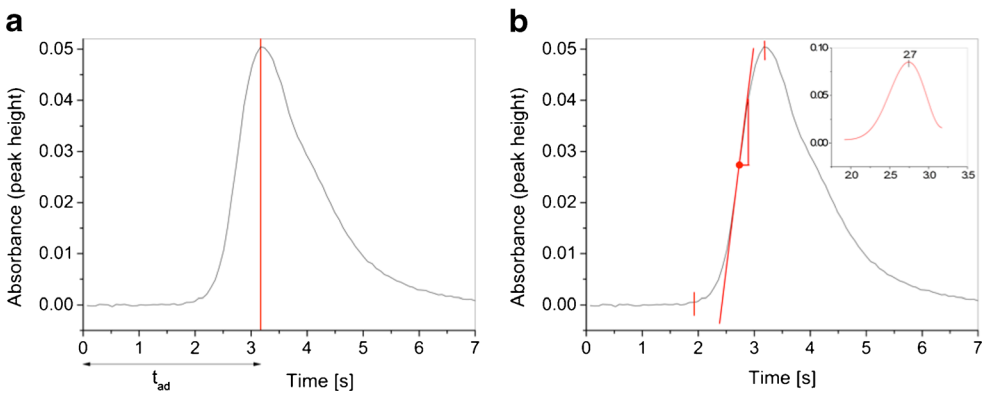

Fig. 2 Exemplary absorbance signal obtained for Ag^+-containing parsley and illustration of the two different evaluation strategies based on **a** atomisation delay t_{ad} and **b** atomisation rate k_{at} (*inset* in **b**: first derivative of the polynomial fitted curve section $y=a_0+a_1x+a_2x^2+a_3x^3+a_4x^4+a_5x^5+a_6x^6+a_7x^7+a_8x^8+a_9x^9$, where y is the absorption signal, a_{1-9} variables, and x the atomization delay)

Table 2 Experimental plan for the 3^3 factorial design for optimisation of the furnace program (all other furnace parameters were set as given in Table 1)

Atomization temperature [°C]	Atomization heating rate [°C s^{-1}]	Pyrolysis temperature [°C]
1,600	1,500	300
1,800	1,700	500
2,000	1,900	700

the applied furnace program. For parsley containing a mixture of AgNPs/Ag^+, one broad asymmetric peak with t_{nad} ranging from 7.39 to 24.50 s mg^{-1} was observed. (Exemplary images for absorbance signals are presented in Electronic supplementary material Fig. S2). Hence, the occurring difference in t_{nad} of Ag^+ and AgNPs does not lead to a double peak, but to a broadening of the absorbance peak and a timely shift of the peak maximum compared with samples containing Ag^+ as the only silver species. In the following, we will show that this time shift can be used as a significant indication for the presence of nanoparticulate silver in the biological sample.

Comparison of t_{nad} values for each individual furnace program revealed always higher $t_{nad}(Ag^+)$ than t_{nad}(AgNPs/Ag^+) values. For illustration, Fig. 3 presents the t_{nad} values obtained when applying an atomisation temperature of 1,600 °C, 1,800 °C or 2,000 °C, respectively, at fixed heating rate (1,700 °C s^{-1}) and pyrolysis temperature (300 °C). Evaluation of the data proves no significant differences when comparing the different sizes of AgNPs (20, 40, 60, or 80 nm). Hence, in the following evaluations, the four AgNP/Ag^+-spiked parsley samples were considered as one set of data. The generally lower t_{nad}(AgNPs/Ag^+) value in comparison to $t_{nad}(Ag^+)$ suggests that atomisation of AgNPs takes place before silver ions were atomised. This finding seems contradictory to results recently published by Gagné et al. [24] who observed a double peak for a mixture of Ag^+ and AgNPs where silver ions were faster atomised than AgNPs. However, they investigated liquid homogenates of rainbow trout liver that contained AgNPs and/or Ag^+, whereas in this work a direct investigation of the solid biological sample was performed. Presumably, matrix effects cause the observed difference in the behaviour of the silver species. This assumption was confirmed by the results we obtained when measuring dissolved ionic and nanoparticulate silver in our standard solutions ($t_{ad}(Ag^+)$=2.38±0.16 s; t_{ad}(20/80-nm-Ag-NPs)= 2.52±0.05 s). Hence, these values obtained by investigation of liquid samples are in perfect accordance to the findings of Gagné et al. [24]. Apparently, Ag^+ ions interact much more with the biological matrix, e.g. form strong bonds with sulfur-containing proteins or other biomolecules than the citrate-coated AgNPs. Due to the low pretreatment temperatures applied for pyrolysis, degradation of the biological matrix in the oven is definitely not complete before the atomisation step starts. As a result, more thermal energy is required to atomise

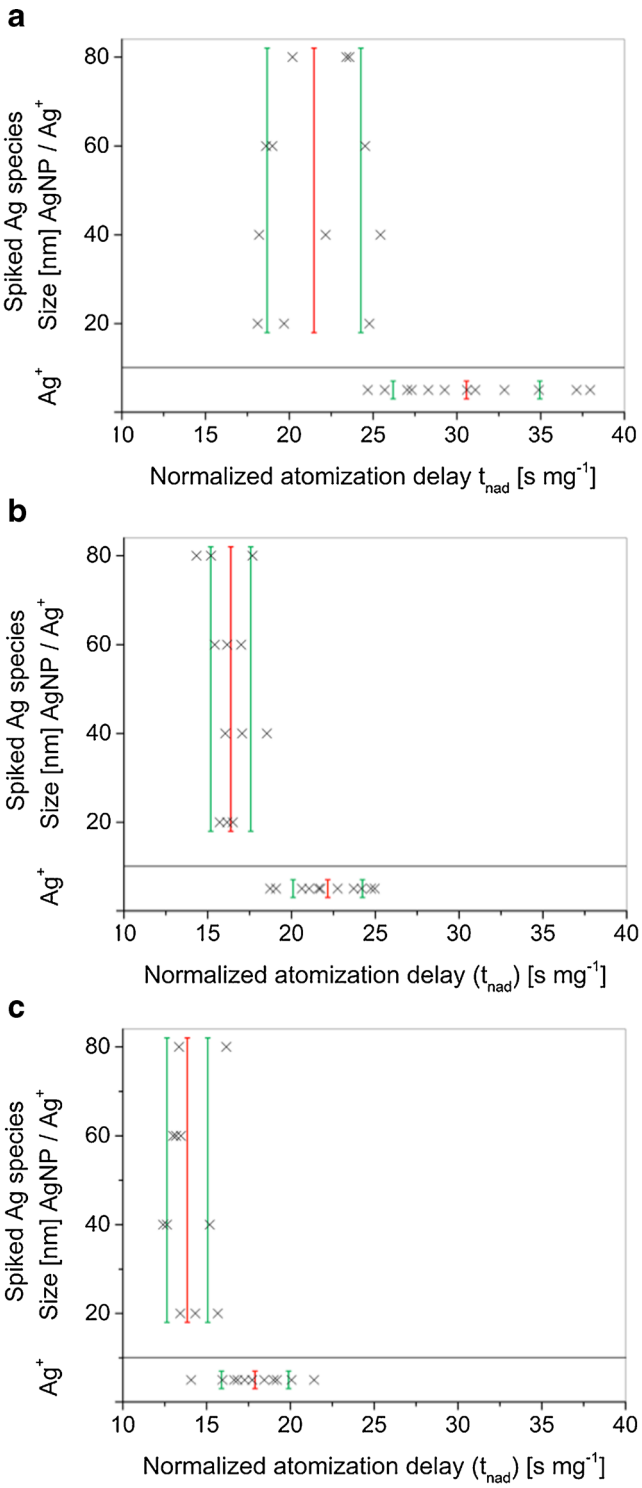

Fig. 3 Normalised atomisation delays (t_{nad}) obtained by application of 1,700 °C s^{-1} heating rate, 300 °C pyrolysis temperature and atomisation temperature of **a** 1,600 °C, **b** 1,800 °C and **c** 2,000 °C to parsley spiked with a mixture of AgNP/Ag^+ or ionic silver only, respectively. *Red lines* represent mean atomisation delays and *green lines* derive from ±1 standard deviation (n=12)

ionic silver from the parsley samples. In agreement with this theory, we observed that the difference in average atomisation delay between Ag^+-spiked parsley and AgNP/Ag^+-spiked parsley is becoming smaller when atomisation temperature is increased (see Fig. 4).

Figure 4 shows the calculated differences (Δt) for the t_{nad} values of Ag^+ and mixtures of AgNPs/Ag^+ for the different furnace programs. The highest difference in atomisation delay (Δt_{nad}=8.02±4.65 s mg^{-1}) was obtained when applying the lowest atomisation temperature (1,600 °C) at the highest heating rate (1,900 °C s^{-1}) and 300 °C pyrolysis temperature (#1 in Fig. 4a). However, evaluation of the results reveals that a significant difference in the atomisation delay of ionic silver to mixtures of AgNPs/Ag^+ is only obtained for the furnace programs #4, 5 and 6 in Fig. 4a ($p<1\times10^{-6}$; P=95 %). Among these furnace programs, #5 gives the highest Δt of 6.27±0.96 s mg^{-1} and is so selected as the optimum program in order to indicate the presence of AgNPs in the biological sample.

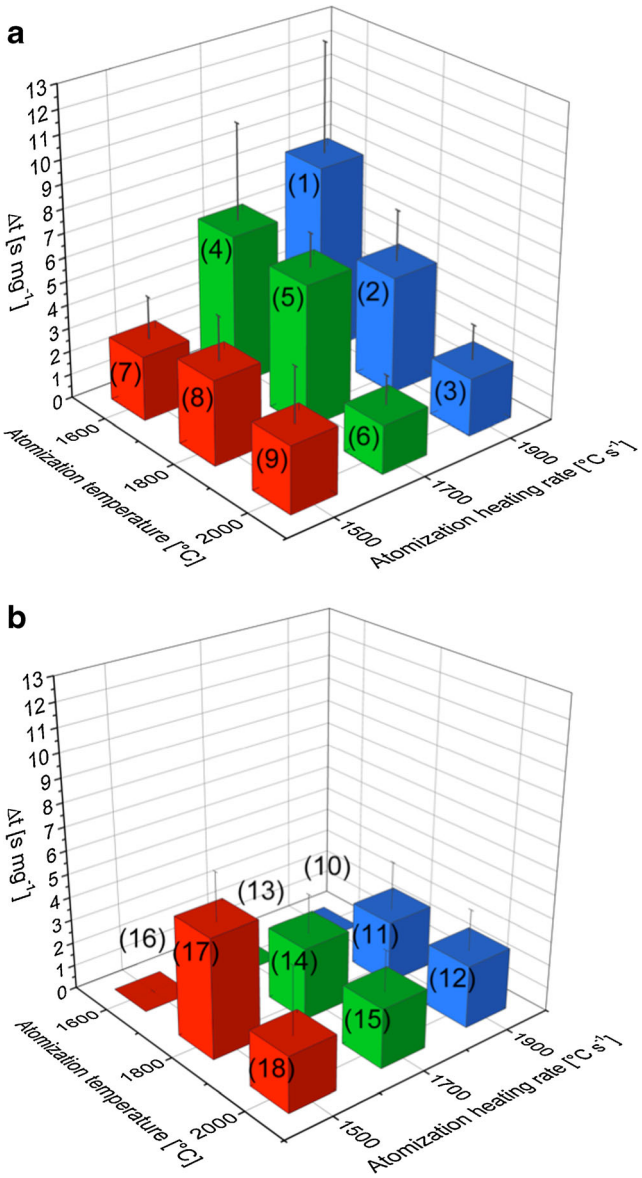

Fig. 4 Mean values for Δt depending on atomisation temperature and atomisation heating rate at a fixed pyrolysis temperature of **a** 300 °C and **b** 500 °C. (*Error bars* represent ±1 standard deviation with n=12; *Numbers in brackets* identify the furnace program; no data available for furnace programs #10, 13 and 16)

Atomisation delay can be interpreted as the actual temperature needed to atomise the main part of silver atoms from the sample, whereas the atomisation rate (k_{at}) could be described as the number of atoms that are atomised per second. It is expected that AgNPs at different sizes and Ag^+ ions will show different k_{at}. In theory, two aspects may influence the atomisation rate: (1) Larger silver particles (assembly of several 100 silver atoms) produce more free atoms at a time; (2) The larger the silver particles are, the slower the heat is transferred. For evaluation of k_{at} from silver-spiked parsley, we examined the slope at the inflection point of the polynomial fitted first section of the absorbance peak (see description above and Fig. 2b). These results obtained by applying furnace program #5 are illustrated in Fig. 5.

As already observed for t_{nad}, the presence of AgNPs gives also significantly different k_{at} values. Generally higher atomisation rates are obtained for parsley spiked with AgNPs/Ag^+-mixtures compared with samples spiked with silver ions only. In addition, evident differences in k_{at} values for different nanoparticle sizes were noticed. A non-linear decrease in k_{at} was found with increasing silver particle size. Moreover, significant differences between k_{at} values for samples spiked with nanoparticle sizes of 20 and 60 nm (p=0.0363; P=95 %), 20 and 80 nm (p=0.0009; P=95 %) and 60 and 80 nm (p=0.0025; P=95 %) were obtained. For 40-nm nanoparticles, no distinct correlations can be drawn due to the relatively high uncertainty.

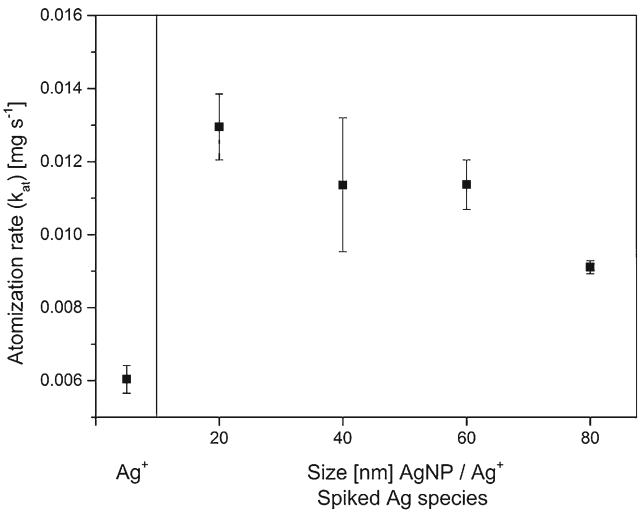

Fig. 5 Atomisation rates k_{at} for the observed absorbance signals for parsley samples spiked with different silver nanoparticle sizes (20, 40, 60 or 80 nm) and Ag^+ obtained by applying furnace program #5. (*Error bars* represent ±1 standard deviation from replicate measurements, n=3)

Conclusions

In this study, we could prove the concept that silver nanoparticles can be directly identified and distinguished from ionic silver in biological samples by means of solid sampling HR-CS AAS. For this purpose, new evaluation strategies for the obtained absorbance signals were developed, and the furnace program was optimised in a multivariate experimental design. The atomisation delay normalised by the sample weight (t_{nad}) was found to be a significant indicator for the presence of AgNPs in parsley samples. A difference of 6.27±0.96 s mg^{-1} in the t_{nad} values was obtained when comparing AgNP-containing parsley with samples that contained ionic silver only. Hence, easy and fast assessment on the presence or absence of AgNPs in the parsley samples is possible by measuring the time delays for the absorbance maximum. Moreover, for AgNP-spiked parsley size distinction between 20-, 60- and 80-nm AgNPs was possible when determining the atomisation rate k_{at}, i.e. the slope of the polynomial fitted curve section of the absorbance signal at the first inflection point. These novel approaches may provide a valuable tool for developing new screening tests for metal NPs in food and environmental samples. Thereby, the presence of metal NPs could be directly investigated in solid samples omitting any time-consuming sample pretreatment steps, like extraction or matrix digestion. In this regard, further experiments on other metal NPs and matrixes shall reveal the general applicability of the approach. Moreover, development of suitable calibration and evaluation strategy for simultaneous quantification of silver in the solid biological samples is planned.

Acknowledgements We would like to express our gratitude to Analytik Jena AG (Jena, Germany) for provision of the high-resolution–continuum source atomic absorption spectrometer *ContrAA600*.

References

1. Lohse SE, Murphy CJ (2012) Applications of colloidal inorganic nanoparticles: from medicine to energy. J Am Chem Soc 134:15607–15620
2. Roco MC (2005) Environmentally responsible development of nanotechnology. Environ Sci Technol 39:106A–112A
3. Prabhu S, Poulose EK (2012) Silver nanoparticles: mechanism of antibacterial action, synthesis, medical applications, and toxicity effects. Int Nano Lett 2:32–42
4. Ahamed M, AlSalhi MS, Siddiqui MKJ (2010) Silver nanoparticle applications and human health. Clin Chim Acta 411: 1841–1848
5. Chaudry Q, Scotter M, Blackburn J, Ross B, Boxall A, Castle L, Aitken R, Watkins R (2008) Applications and implications of nanotechnologies for the food sector. Food Addit Contam 25:241–258
6. Reidy B, Haase A, Luch A, Dawson KA, Lynch I (2013) Mechanism of silver nanoparticle release, transformation and toxicity: a critical review of current knowledge and recommendations for future studies and applications. Materials 6:2295–2350
7. Cushen M, Kerry J, Morris M, Cruz-Romero M, Cummins E (2012) Nanotechnologies in the food industry—recent developments, risks and regulation. Trends Food Sci Technol 24:30–46
8. Faunce T, Watal A (2010) Nanosilver and global public health: international regulatory issues. Nanomedicine 5:617–632
9. Wijnhoven SWP, Peijnenburg WJGM, Herberts CA, Hagens W, Oomen AG, Heugens EHV, Roszek B, Bisschops J, Gosens I, van de Meent D (2009) Nano-silver—a review of available data and knowledge gaps in human and environmental risk assessment. Nanotoxicology 3:109–138
10. Huang Y, Chen S, Bing X, Gao C, Wang T, Yuan B (2011) Nanosilver migrated into food-simulating solutions from commercially available food fresh containers. Packag Technol Sci 24:291–297
11. Kim T-H, Kim M, Park H-S, Shin US, Gog M-S, Kim H-W (2012) Size-dependent cellular toxicity of silver nanoparticles. J Biomed Mater Res 100A:1033–1043
12. Asghari S, Johari SA, Lee JH, Kim YS, Jeon YB, Choi HJ, Moon MC, Yu IJ (2012) Toxicity of various silver nanoparticles compared to silver ions in *Daphnia magna*. J Nanobiotechnol 10:14–24
13. Sung JH, Ji JH, Park JD, Yoon JU, Kim DS, Jeon KS, Song MY, Jeong J, Han BS, Han JH, Chung YH, Chang HK, Lee JH, Cho MH, Kelman BJ, Yu IJ (2009) Subchronic inhalation toxicity of silver nanoparticles. Toxicol Sci 108:452–461
14. Van Aerle R, Lange A, Moorhouse A, Paszkiewicz K, Ball K, Johnston BD, de Bastos E, Booth T, Tyler CR, Santos EM (2013) Molecular mechanisms of toxicity of silver nanoparticles in zebrafish embryos. Environ Sci Technol 47:8005–8014
15. Yen H-J, Hsu S-H, Tsai C-L (2009) Cytotoxicity and immunological response of gold and silver nanoparticles of different sizes. Small 5: 1553–1561
16. Eom H-J, Choi J (2010) p38 MAPK activation, DNA damage, cell cycle arrest and apoptosis as mechanism of toxicity of silver nanoparticles in Jurkat T cells. Environ Sci Technol 44: 8337–8342
17. Hussain SM, Hess KL, Gearhart JM, Geiss KT, Schlager JJ (2005) In vitro toxicity of nanoparticles in BRL 3A rat liver cells. Toxicol In Vitro 19:975–983
18. Medina C, Santos-Martinez MJ, Radomski A, Corrigan OI, Radomski MW (2007) Nanoparticles: pharmacological and toxicological significance. Br J Pharmacol 150:552–558
19. Oberdörster G, Sharp Z, Atudorei V, Elder A, Gelein R, Kreyling W, Cox C (2004) Translocation of inhaled ultrafine particles to the brain. Inhal Toxicol 16:437–445
20. Loeschner K, Navratilova J, Købler C, Mølhave K, Wagner S, von der Kammer F, Larsen EH (2013) Detection and characterization of silver nanoparticles in chicken meat by asymmetric flow field flow fractionation with detection by conventional or single particle ICP-MS. Anal Bioanal Chem 405:8185–8195
21. Mitrano DM, Lesher EK, Bednar A, Monserud J, Higgins CP, Ranville JF (2012) Detecting nanoparticulate silver using single-particle inductively coupled plasma-mass spectrometry. Environ Toxicol Chem 31:115–121
22. Zhang Z, Kong F, Vardhanabhuti B, Mustapha A, Lin M (2012) Detection of engineered silver nanoparticle contamination in pears. J Agric Food Chem 60:10762–10767
23. Rebe Raz S, Leontaridou M, Bremer MGEG, Peters R, Weigel S (2012) Development of surface plasmon resonance-based sensor for detection of silver nanoparticles in food and the environment. Anal Bioanal Chem 403:2843–2850
24. Gagné F, Turcotte P, Gagnon C (2012) Screening test of silver nanoparticles in biological samples by graphite furnace atomic absorption spectrometry. Anal Bioanal Chem 404:2067–2072

25. Chao J-B, Liu J-F, Yu S-J, Feng Y-D, Tan Z-Q, Liu R, Yin Y-G (2011) Speciation analysis of silver nanoparticles and silver ions in antibacterial products and environmental waters via cloud point extraction-based separation. Anal Chem 83:6875–6882

26. Dittert IM, Borges DLG, Welz B, Curtius AJ, Becker-Ross H (2009) Determination of silver in geological samples using high-resolution continuum source electrothermal atomic absorption spectrometry and direct solid sampling. Michrochim Acta 167:21–26